Improving Spatially Coupled LDPC Codes by Connecting Chains

Truhachev, Dmitri; Mitchell, David G.M.; Lentmaier, Michael; Costello Jr., Daniel J.

Published in:
2012 IEEE International Symposium on Information Theory Proceedings

DOI:
10.1109/ISIT.2012.6284232

2012

Improving Spatially Coupled LDPC Codes by Connecting Chains

Dmitri Truhachev*, David G. M. Mitchell†, Michael Lentmaier‡, and Daniel J. Costello, Jr.†
*Department of Computing Science, University of Alberta, Edmonton, Canada
dmitryt@ualberta.ca
†Dept. of Electrical Engineering, University of Notre Dame, Notre Dame, Indiana, USA,
{david.mitchell, costello.2}@nd.edu
‡Vodafone Chair Mobile Communications Systems, Dresden University of Technology, Dresden, Germany,
michael.lentmaier@ifn.et.tu-dresden.de

***Abstract*—In this paper, we study ensembles of connected spatially coupled low-density parity-check codes (SC-LDPCCs), i.e., ensembles described by graphs in which regular SC-LDPCC chains of various lengths serve as edges. We show that, by carefully connecting individual SC-LDPCC chains, we obtain LDPC code ensembles with improved iterative decoding thresholds compared to those of a single coupled chain, in addition to reducing the decoding complexity required to achieve a specific bit error probability. Moreover, we show that, like the component SC-LDPCC chains, the proposed constructions have a typical minimum distance that grows linearly with block length.**

I. Introduction

Recently, iterative processing on *spatially coupled* sparse graphs has received a lot of attention in the literature. The concept of coupling a sequence of identical small structured graphs into a chain with improved properties, first demonstrated in the context of low-density parity-check (LDPC) convolutional codes [1], has been shown to be applicable to a diverse list of topics, such as compressed sensing [2], multiuser communication [3] [4], quantum codes [5], relay channels [6], [7], wiretap channels [8], and models in statistical physics [9].

Ensembles of spatially coupled LDPC codes (SC-LDPCCs) can be obtained by terminating regular LDPC convolutional code ensembles [10]. The slight irregularity resulting from the termination of the convolutional codes has been shown to lead to substantially better belief propagation (BP) decoding thresholds compared to corresponding block, or *uncoupled*, code ensembles for a variety of channels [10]–[13]. Further, it has recently been proven analytically for the binary erasure channel (BEC) that the BP decoding thresholds of a class of regular SC-LDPCC ensembles approach the maximum a posteriori (MAP) decoding thresholds of the corresponding LDPC block code ensembles [14].

In this work, we extend the results presented in [15], [16] and show that by carefully connecting individual SC-LDPCC chains, we can obtain LDPC code ensembles with improved iterative decoding thresholds for a wide variety of rates. Communication over the binary erasure channel (BEC) and the additive white Gaussian noise (AWGN) channel have been considered. Moreover, we show that this new code construction also decreases the decoding complexity required to achieve specific decoding error probabilities in the near threshold region. Finally, we show that the constructed ensembles, like the individual component SC-LDPCC chains, are *asymptotically good*, i.e., they have the property that their minimum distance increases linearly with block length.

This work was partially supported by NSF Grants CCF-0830650 and CCF-1161754, and the Alberta Innovates Fund.

II. Code Construction

A *protograph* [17] is a small Tanner graph described by an $n_c \times n_v$ incidence matrix $\mathbf{B}$, known as a base matrix, that consists of non-negative integers $B_{i,j}$ that correspond to $B_{i,j}$ parallel edges in the graph. A protograph-based code is obtained by taking an M-fold graph cover of a given protograph and can be described by an $Mn_c \times Mn_v$ parity-check matrix obtained by replacing each non-zero entry $B_{i,j}$ by a sum of $B_{i,j}$ non-overlapping permutation matrices of size $M \times M$ and a zero entry by the $M \times M$ all-zero matrix. Therefore, a protograph with a *lifting factor* of M describes an ensemble of LDPC codes.

A. SC-LDPCC Ensembles

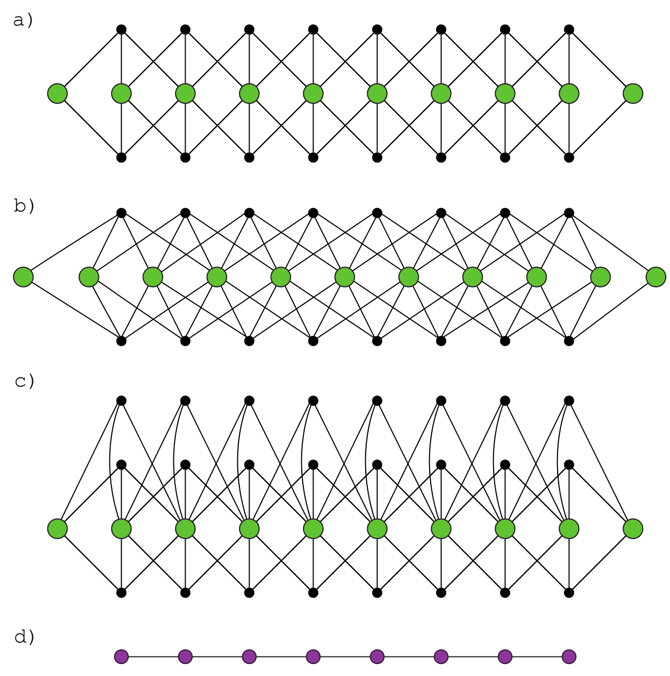

Fig. 1. The protographs of several SC-LDPCC chains of length $L = 8$: (a) $(3, 6)$-regular, (b) $(4, 8)$-regular, (c) $(3, 9)$-regular, and (d) their simplified representation.

A protograph of a $(3, 6)$-regular SC-LDPCC chain of length $L = 8$ is depicted in Fig. 1(a). The green circles in the figure illustrate check nodes and the black circles illustrate variable nodes. Note that each variable node is connected to 3 parity check nodes, while the parity check nodes in the middle are connected to 6 variable nodes. The check nodes located at the beginning and at the end of the chain, however, are only connected to either 2 or 4 variable nodes. Figs. 1(b) and (c) show the coupling concept for $(4, 8)$- and $(3, 9)$-regular graphs, respectively. A simplified illustration of the protographs of a length $L = 8$ chain is given in Fig. 1(d). Each magenta node illustrates a segment of the (J, K)-regular SC-LDPCC chain. We will denote the ensemble associated with a (J, K)-regular SC-LDPCC chain of length L by $\mathcal{C}(J, K, L)$.

B. Connecting Two Coupled Chains: The Loop

In this paper, we will construct the protograph of an LDPC code ensemble by interconnecting the protographs of two (J, K)-regular SC-LDPCC chains.[1] The connected protograph, depicted in Fig. 2, is called the *loop* and is denoted by $\mathcal{L}(J, K, L)$. Here, the last segment of chain one is connected to an inner segment of chain two, while the first segment of chain two is connected to an inner segment of chain one. It was shown in [16] that, when connecting SC-LDPCC chains, the performance is sensitive to the position of the connecting points. In this paper, we will connect the chains at positions $\max(2, \lfloor L/3 \rfloor)$. The particular connections made between the chains will vary depending on the component chains, and we will see in Section IV that the threshold and speed of convergence can be improved by carefully choosing where to place the connecting edges.

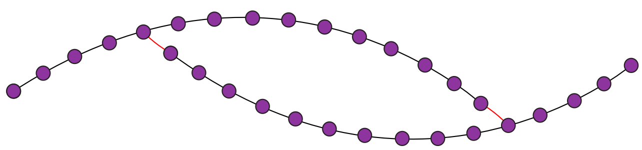

Fig. 2. Two connected (J, K)-regular SC-LDPCC chains of length $L = 15$.

III. Analysis of Connected SC-LDPCCs

A. Iterative Decoding Analysis

The analysis of the iterative decoding performance of codes described by protographs can be obtained via density evolution, which, for the case of the BEC, is explained as follows.

We denote the set of variable nodes connected to check node k in the protograph by $\mathbb{V}(k)$ and the set of check nodes connected to variable node j by $\mathbb{C}(j)$. The probability that the message passed from check node k to variable node j in iteration i is an erasure is denoted by $q_{kj}^{(i)}$. The probability of an erasure message from variable node j to check node k is similarly denoted by $p_{jk}^{(i)}$. The following equations relate the erasure probabilities of the messages at different iterations:

$$q_{kj}^{(i)} = 1 - \prod_{j' \in \mathbb{V}(k) \setminus j} (1 - p_{j'k}^{(i-1)}) \ , \tag{1}$$

$$p_{jk}^{(i)} = \epsilon \prod_{k' \in \mathbb{C}(j) \setminus k} q_{k'j}^{(i)} \ . \tag{2}$$

The variable node messages are initialized as $p_{jk}^{(0)} = \epsilon$ at iteration 0. The bit error probability of variable node j at iteration i can be calculated as

$$P_{\mathrm{b}}(j) = \epsilon \prod_{k \in \mathbb{C}(j)} q_{kj}^{(i)} \ . \tag{3}$$

[1]Constructions consisting of more than two connected chains are also possible [15], [16].

B. Asymptotic Minimum Distance Analysis

In [18], Divsalar presented a technique to calculate the average weight enumerator for protograph-based block code ensembles. This weight enumerator can be used to test if an ensemble is *asymptotically good*, i.e., if the minimum distance typical of most members of the ensemble is at least as large as $\delta_{min} n$, where $\delta_{min} > 0$ is the *minimum distance growth rate* of the ensemble and n is the block length. In [19], it was shown that ensembles of (J, K)-regular SC-LDPCCs (i.e., individual chains) are asymptotically good. In Section IV, we present the results of a similar protograph-based analysis for ensembles of connected SC-LDPCCs to see if they share the good distance properties of the individual chains.

IV. Results

In this section, we present the iterative decoding threshold and asymptotic minimum distance results obtained for several SC-LDPCC loop ensembles. We will first show that the $\mathcal{L}(J, 2J, L)$ loop ensembles have the same rate but better thresholds than the individual $\mathcal{C}(J, 2J, L)$ ensembles. We then proceed to show that this same improvement is visible as we increase the rate of the component SC-LDPCC chains.

A. The $(3, 6)$ SC-LDPCC Loop Ensemble $\mathcal{L}(3, 6, L)$

The first component chain we consider is the $(3, 6)$-regular SC-LDPCC chain shown in Fig. 1(a). We take two of these chains and connect them together as shown in Fig. 2. The connections are made as shown in Fig. 3. Note that, at the connection points, the two check nodes at the end of the chain have an additional 2 and 4 edges (shown in red) that connect to the variable nodes of the adjacent chain. As a result, the loop construction $\mathcal{L}(3, 6, L)$ has reduced check node degrees only at the open ends of the loop. However, at each connection point, there are 6 variable nodes that have degree 4. Consequently, for the loop ensemble $\mathcal{L}(3, 6, L)$, the average check node degree is $6(L + 1)/(L + 2)$ and the average variable node degree is $3(L+1)/L$. We note that, just as in the case of a single $(3, 6)$-regular SC-LDPCC chain, the degree distribution approaches that of a $(3, 6)$-regular code as L grows. The rates of both the loop ensemble $\mathcal{L}(3, 6, L)$ and the single chain ensemble $\mathcal{C}(3, 6, L)$ are equal and are given by $R_L = (L - 2)/2L$.

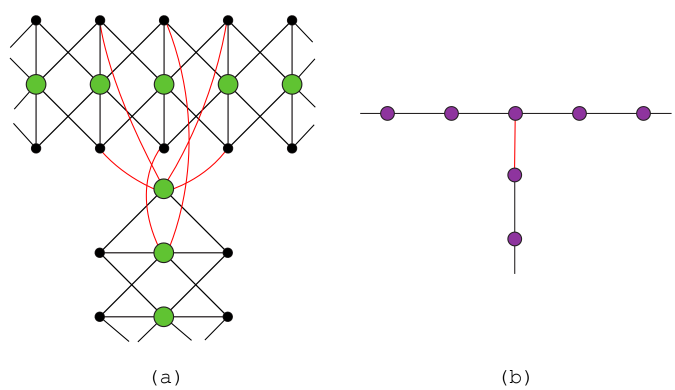

Fig. 3. Graphs depicting (a) two connected spatially coupled $(3, 6)$-regular protograph chains, and (b) the simplified representation. The connecting edges are shown in red.

Fig. 4 shows the calculated BEC thresholds for the $\mathcal{L}(3,6,L)$ ensembles in comparison to the $\mathcal{C}(3,6,L)$ and $\mathcal{C}(4,8,L)$ single chain ensembles for a variety of chain lengths L. Comparing the $\mathcal{L}(3,6,L)$ ensembles to the $\mathcal{C}(3,6,L)$ ensembles, we observe that, for $L > 5$, the thresholds of the loop ensembles are generally superior with the exception of large L. In particular, we observe a dramatic threshold improvement for ensembles with rates in the region $0.3571 \leq R_L \leq 0.4375$. For large values of L, the improvement diminishes. The thresholds of the single chain ensembles $\mathcal{C}(3,6,L)$ and $\mathcal{C}(4,8,L)$ can be observed to converge to values close to the MAP threshold of the underlying (J,K)-regular LDPC code as L becomes sufficiently large. (Recall that it has been shown in [14] that the BP thresholds of a class of SC-LDPCC ensembles on the BEC are equal to the (optimal) MAP thresholds of their corresponding LDPC block code ensembles.) As a result, for large L, we observe the surprising behaviour that the iterative decoding thresholds of the $\mathcal{C}(4,8,L)$ ensembles are larger than the $\mathcal{C}(3,6,L)$ thresholds (unlike the corresponding LDPC block code ensembles). However, even in this region, we observe that the thresholds of the $\mathcal{L}(3,6,L)$ ensemble remain above the $\mathcal{C}(4,8,L)$ thresholds for rates between 0.4 and 0.45. In the next section, we will see that a loop constructed using $(4,8)$-regular SC-LDPCC chains achieves further performance improvement.

AWGN channel thresholds for the loop ensembles $\mathcal{L}(3,6,L)$ are given in Table I for $L = 12, 15$, and 18. The results for the single chain ensembles $\mathcal{C}(3,6,L)$ are shown for comparison. We notice that the thresholds of the loop ensembles are significantly better than these for corresponding single chains.

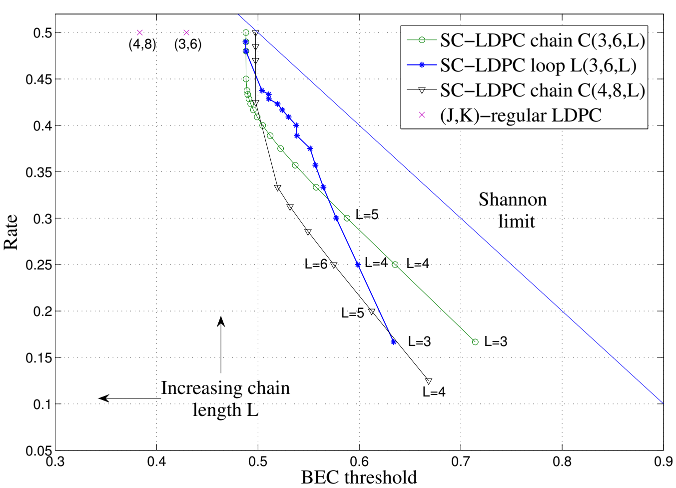

Fig. 4. BEC thresholds calculated for the $\mathcal{L}(3,6,L)$ loop ensembles as well as some $\mathcal{C}(J,K,L)$ ensembles and (J,K)-regular LDPCC ensembles.

In addition to an improvement in threshold, we also find that connecting two chains may improve the speed of convergence of the chains at the connecting points. The evolution of the bit error probability for the variable nodes of the loop ensemble $\mathcal{L}(3,6,15)$ is illustrated in Fig. 5. The red curves correspond to the error probability at each node position at iterations $1, 6, 11, \ldots, 36$ (from top to bottom). The green curves correspond to the error probability as a function of

Rate	Ensemble	$(E_b/N_0)^*$	Ensemble	$(E_b/N_0)^*$
0.4167	$\mathcal{L}(3,6,12)$	0.6520dB	$\mathcal{C}(3,6,12)$	1.1167dB
0.4333	$\mathcal{L}(3,6,15)$	0.7281dB	$\mathcal{C}(3,6,15)$	1.0431dB
0.4444	$\mathcal{L}(3,6,18)$	0.7850dB	$\mathcal{C}(3,6,18)$	0.9659dB

TABLE I
AWGN CHANNEL THRESHOLDS $(E_B/N_0)^*$ CALCULATED FOR THE $\mathcal{L}(3,6,L)$ LOOP ENSEMBLES AND THE $\mathcal{C}(3,6,L)$ ENSEMBLES FOR $L = 12$, 15, AND 18.

the node position for the single chain ensemble $\mathcal{C}(3,6,15)$ and iteration numbers $1, 6, 11, \ldots, 36$. The BEC erasure probability is fixed to be 0.488. We note that the red curves achieve low bit error probabilities much faster than the green curves. In addition, it takes fewer decoding iterations for the loop ensemble $\mathcal{L}(3,6,15)$ to converge to a given bit error probability.

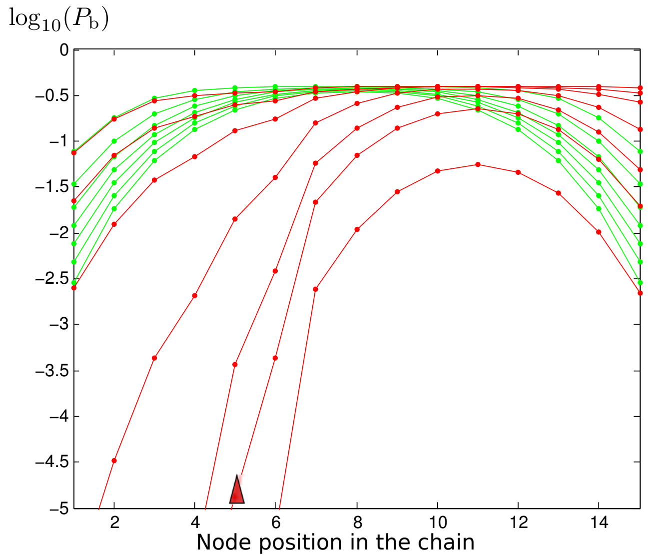

Fig. 5. Logarithm of the bit error probability for the variable nodes of a) chain one of the ensemble $\mathcal{L}(3,6,15)$ (red curves), and b) ensemble $\mathcal{C}(3,6,15)$ (green curves), as a function of the position of the node in the chain. The curves (either red or green) are computed for decoding iterations $1, 6, 11, \ldots, 36$ (from top to bottom). The position where chain one is connected to the end of chain two is shown by the red triangle.

Fig. 6 shows the asymptotic minimum distance growth rates calculated for the $\mathcal{L}(3,6,L)$ ensembles as well as some $\mathcal{C}(J,2J,L)$ ensembles and (J,K)-regular LDPCC ensembles. In addition to their good threshold performance, the $\mathcal{L}(3,6,L)$ ensembles were found to be asymptotically good for all tested values of L. As the chain length L increases, the rate increases and the minimum distance growth rates decrease for all the SC-LDPCC ensembles. We observe that, for short chain lengths $L = 3, 4, 5$, the $\mathcal{L}(3,6,L)$ ensembles display distance growth rates similar to the $\mathcal{C}(4,8,L)$ ensembles, and much larger than the $\mathcal{C}(3,6,L)$ ensembles. This can be explained in part by the increased variable node degrees (the average variable node degrees are 4, 3.75, and 3.6, respectively, while the average check node degrees are 4.8, 5, and 5.1429, respectively). For $L > 5$, as the thresholds of the $\mathcal{L}(3,6,L)$ ensembles exceed the thresholds of the $\mathcal{C}(3,6,L)$ ensembles, we see that the distance growth rates display the opposite behaviour. Finally, as $L \to \infty$ the minimum distance growth rates decrease and tend to zero as $L \to \infty$.

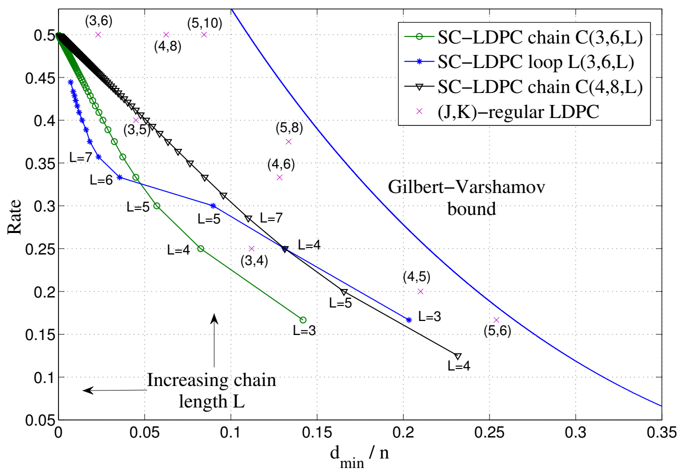

Fig. 6. Asymptotic minimum distance growth rates calculated for the $\mathcal{L}(3,6,L)$ loop SC-LDPCC ensembles as well as some $\mathcal{C}(J,K,L)$ SC-LDPCC ensembles and (J,K)-regular LDPCC ensembles.

B. The $(4,8)$ SC-LDPC Loop Ensemble $\mathcal{L}(4,8,L)$

We now proceed to form a loop consisting of two $(4,8)$-regular SC-LDPCC chains. The individual chains are shown in Fig. 1(b). We consider two different ways to connect the chains, depicted in Fig. 7. The first, shown in Fig. 7(a), has an additional 12 edges added at the connecting point. Here, the check nodes at the connection all have degree 8, while the 6 connecting variable nodes of chain one have degree 6. The second connection, depicted in Fig. 7(b), introduces 6 additional edges and connects them in a similar fashion to the $(3,6)$ chains. As a result, the 3 check nodes at the connecting end of chain two have degree 6, and the 6 connecting variable nodes of chain one have degree 5. We denote the ensembles connected using Fig. 7(a) by $\mathcal{L}^A(4,8,L)$ and the ensembles connected using Fig. 7(b) by $\mathcal{L}^B(4,8,L)$.

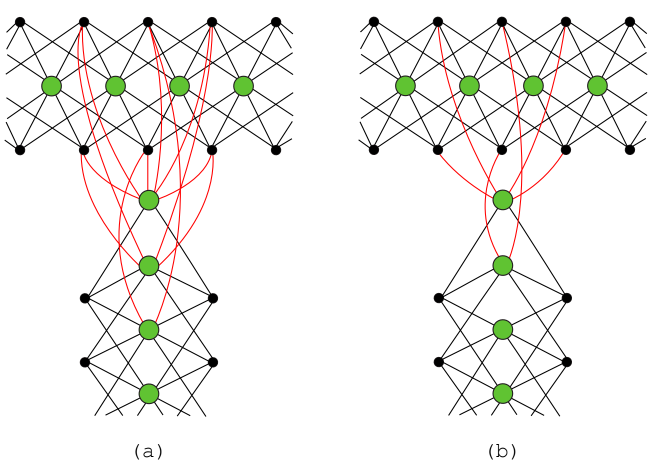

Fig. 7. Connected spatially coupled $(4,8)$-regular protograph chains. The connecting edges are shown in red.

BEC thresholds calculated for the ensembles $\mathcal{L}^A(4,8,L)$ and $\mathcal{L}^B(4,8,L)$ are given in Table II, as well at the thresholds calculated for the single chain ensemble $\mathcal{C}(4,8,L)$. We see that the thresholds of the ensembles with connection B (fewer connecting edges) are always at least as large as the thresholds for connection A, with equality occurring for large chain length L. We see the same behaviour as for the $(3,6)$ loops: for short L and low rates, the ensemble $\mathcal{C}(4,8,L)$ has the largest threshold; for a large rate region in the middle of the achievable range, the loop ensembles have significantly better thresholds; and, finally, the improvement observed for the loop ensembles diminishes as L becomes large and the thresholds converge at a value slightly below the MAP threshold of the underlying ensemble. The threshold difference between ensembles $\mathcal{L}^A(4,8,L)$ and $\mathcal{L}^B(4,8,L)$ indicates that the performance is sensitive to the choice of additional edges connecting the chains.

L	R	$\mathcal{L}^A(4,8,L)$	$\mathcal{L}^B(4,8,L)$	$\mathcal{C}(4,8,L)$
6	0.2500	0.5629	0.5709	0.5748
9	0.3333	0.5342	0.5399	0.5194
12	0.3750	0.5185	0.5247	0.5021
15	0.4000	0.5088	0.5138	0.4983
75	0.4800	0.4975	0.4975	0.4977
150	0.4900	0.4971	0.4971	0.4977

TABLE II
BEC THRESHOLDS FOR SC-LDPCC LOOP ENSEMBLES $\mathcal{L}^A(4,8,L)$ AND $\mathcal{L}^B(4,8,L)$ AND THE SINGLE CHAIN SC-LDPCC ENSEMBLE $\mathcal{C}(4,8,L)$.

Fig. 8 shows the evolution of the bit error probability for the variable nodes of chain one for the ensembles $\mathcal{L}^A(4,8,12)$ (blue curves) and $\mathcal{L}^B(4,8,12)$ (red curves). The BEC erasure probability is fixed to be 0.514, and error probabilities are plotted for iteration numbers $1,6,11,\ldots,56$. We observe that the red curves (corresponding to fewer additional edges at the connecting points) achieve low bit error probabilities much faster than the blue curves, i.e., in addition to improved thresholds, connection method B also enables faster convergence to a specific bit error probability.

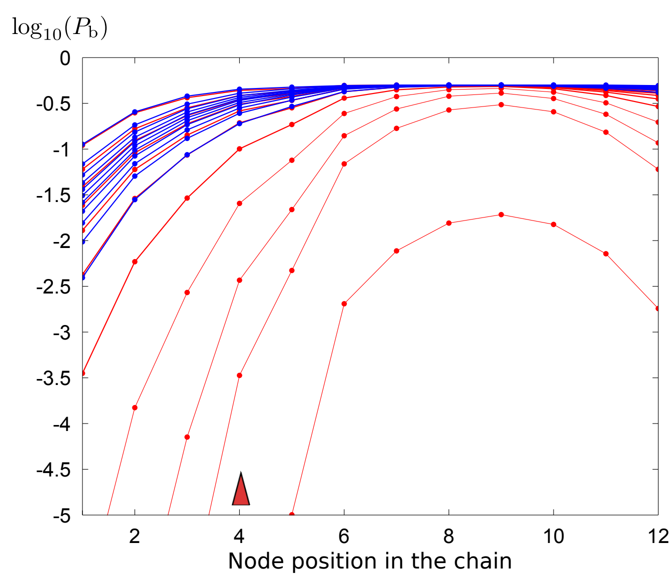

Fig. 8. Logarithm of the bit error probability for the variable nodes of chain one of the ensembles $\mathcal{L}^A(4,8,12)$ (blue curves) and $\mathcal{L}^B(4,8,12)$ (red curves), as a function of the position of the node in the chain. The curves (either blue or red) are computed for decoding iterations $1,6,11,\ldots,56$ (from top to bottom). The position where chain one is connected to the end of chain two is shown by the red triangle.

C. The $(3,9)$ SC-LDPCC Loop Ensemble $\mathcal{L}(3,9,L)$

As a final example, we construct some higher rate loop ensembles by connecting two $(3,9)$-regular SC-LDPCC chains. As a result of the boundary effects of spatial coupling, there is some rate loss for finite chain length L. Consequently, a code designer may be tempted to choose a large chain length L, where the design rate of the ensemble is higher and the threshold is closer to capacity. However, the performance of the code is also affected by the size of the lifting factor M and, for a fixed block length, practical limitations may require a moderate choice of L, where the thresholds are typically further from capacity. For high rate coupled ensembles, in the region of moderate values of L, the loop ensembles are particularly promising, since this is where they provide the largest threshold improvement. A $(3,9)$-regular SC-LDPCC chain is shown in Fig. 1(c). We connect the chains as shown in Fig. 9, using the reduced edge type of connection discussed in Section IV-B.

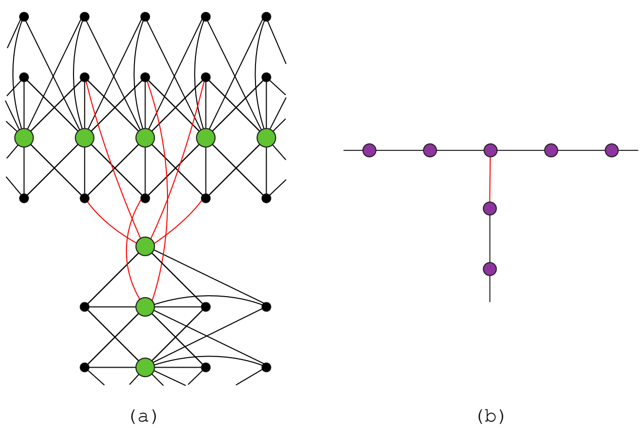

Fig. 9. Graphs depicting (a) two connected spatially coupled $(3,9)$-regular protograph chains, and (b) the simplified representation. The connecting edges are shown in red.

The BEC thresholds calculated for the ensembles $\mathcal{L}(3,9,L)$ and $\mathcal{C}(3,9,L)$ are given in Table III. We see that ensemble $\mathcal{L}(3,9,L)$ has significantly larger thresholds than ensemble $\mathcal{C}(3,9,L)$ for all the moderate values of L tested. Also, we find that the loop ensembles $\mathcal{L}(3,9,L)$ are asymptotically good. For example, we calculate δ_{min} as 0.0063, 0.0036, and 0.0023 for $L=6$, 8, and 12, respectively.

L	R	$\mathcal{L}(3,9,L)$	$\mathcal{C}(3,9,L)$
6	0.5556	0.3746	0.3605
8	0.5883	0.3604	0.3392
12	0.6111	0.3437	0.3235
100	0.6600	0.3191	0.3196

TABLE III
BEC THRESHOLDS FOR THE SC-LDPCC LOOP ENSEMBLE $\mathcal{L}(3,9,L)$ AND THE SINGLE CHAIN SC-LDPCC ENSEMBLE $\mathcal{C}(3,9,L)$.

V. Conclusions

In this paper, we showed that by connecting individual chains of (J,K)-regular SC-LDPCCs we obtain LDPC code ensembles with improved iterative decoding thresholds compared to those of a single coupled chain for a large portion of the achievable rate region. Moreover, we saw that connecting SC-LDPCC chains may also reduce the decoding complexity required to achieve a specific bit error probability. We also showed that, like the component SC-LDPCC chains, the proposed constructions have a typical minimum distance that grows linearly with block length, and there exists a trade-off between the minimum distance growth rate and the iterative decoding threshold for a particular code rate. Finally, we observed that the iterative decoding thresholds and convergence behaviour can be further improved by carefully designing the connections between the chains.

References

[1] A. Jiménez Felström and K. Sh. Zigangirov, "Time-varying periodic convolutional codes with low-density parity-check matrices," *IEEE Trans. Inf. Theory*, vol. 45, no. 6, pp. 2181–2191, Sept. 1999.

[2] S. Kudekar and H. D. Pfister, "The effect of spatial coupling on compressive sensing," in *Proc. Allerton Conference on Communications, Control, and Computing*, Monticello, IL, Sept. 2010.

[3] C. Schlegel and D. Truhachev, "Multiple access demodulation in the lifted signal graph with spatial coupling," in *Proc. IEEE Int. Symp. on Inf. Theory*, St. Petersburg, Russia, Aug. 2011, pp. 2989–2993.

[4] K. Takeuchi, T. Tanaka, and T. Kawabata, "Improvement of BP-based CDMA multiuser detection by spatial coupling," in *Proc. IEEE Int. Symp. on Inf. Theory*, St. Petersburg, Russia, Aug. 2011.

[5] M. Hagiwara, K. Kasai, H. Imai, and K. Sakaniwa, "Spatially coupled quasi-cyclic quantum LDPC codes," in *Proc. IEEE Int. Symp. on Inf. Theory*, St. Petersburg, Russia, Aug. 2011.

[6] Z. Si, R. Thobaben, and M. Skoglund, "Bilayer LDPC convolutional codes for half-duplex relay channels," in *Proc. IEEE International Symposium on Information Theory*, St. Petersburg, Russia, Aug. 2011.

[7] H. Uchikawa, K. Kasai, and K. Sakaniwa, "Spatially coupled LDPC codes for decode-and-forward in erasure relay channel," in *Proc. IEEE Int. Symp. on Inf. Theory*, St. Petersburg, Russia, Aug. 2011.

[8] V. Rathi, R. Urbanke, M. Andersson, and M. Skoglund, "Rate-equivocation optimally spatially coupled LDPC codes for the BEC wiretap channel," in *Proc. IEEE Int. Symp. on Inf. Theory*, St. Petersburg, Russia, Aug. 2011.

[9] S. H. Hassani, N. Macris, and R. Urbanke, "Coupled graphical models and their thresholds," in *Proc. IEEE Inf. Theory Workshop*, Dublin, Ireland, Oct. 2010.

[10] M. Lentmaier, G. P. Fettweis, K. Sh. Zigangirov, and D. J. Costello, Jr., "Approaching capacity with asymptotically regular LDPC codes," in *Proc. Inf. Theory and App. Workshop*, San Diego, CA, Feb. 2009.

[11] M. Lentmaier, A. Sridharan, D. J. Costello, Jr., and K. Sh. Zigangirov, "Iterative decoding threshold analysis for LDPC convolutional codes," *IEEE Trans. Inf. Theory*, vol. 56, no. 10, pp. 5274–5289, Oct. 2010.

[12] M. Lentmaier, D. G. M. Mitchell, G. P. Fettweis, and D. J. Costello, Jr., "Asymptotically good LDPC convolutional codes with AWGN channel thresholds close to the Shannon limit," in *Proc. 6th Int. Symp. on Turbo Codes and Iterative Inf. Processing*, Brest, France, Sept. 2010.

[13] S. Kudekar, C. Méasson, T. Richardson, and R. Urbanke, "Threshold saturation on BMS channels via spatial coupling," in *Proc. 6th Int. Symp. on Turbo Codes and Iterative Information Processing*, Brest, France, Sept. 2010.

[14] S. Kudekar, T. J. Richardson, and R. L. Urbanke, "Threshold saturation via spatial coupling: why convolutional LDPC ensembles perform so well over the BEC," *IEEE Trans. Inf. Theory*, vol. 57, no. 2, pp. 803–834, Feb. 2011.

[15] D. Truhachev, D. G. M. Mitchell, M. Lentmaier, and D. J. Costello, Jr., "Connecting spatially coupled LDPC code chains," in *Proc. IEEE Int. Conf. on Comm.*, Ottawa, Canada, June 2012.

[16] D. Truhachev, D. G. M. Mitchell, M. Lentmaier, and D. J. Costello, Jr., "New codes on graphs constructed by connecting spatially coupled chains," in *Proc. Inf. Theory and App. Workshop*, San Diego, CA, Feb. 2012.

[17] J. Thorpe, "Low-density parity-check (LDPC) codes constructed from protographs," Jet Propulsion Laboratory, Pasadena, CA, INP Progress Report 42-154, Aug. 2003.

[18] D. Divsalar, "Ensemble weight enumerators for protograph LDPC codes," in *Proc. IEEE Int. Symp. on Inf. Theory*, Seattle, WA, July 2006.

[19] M. Lentmaier, D. G. M. Mitchell, G. P. Fettweis, and D. J. Costello, Jr., "Asymptotically regular LDPC codes with linear distance growth and thresholds close to capacity," in *Proc. Inf. Theory and App. Workshop*, San Diego, CA, Feb. 2010.